ACS APPLIED NANO MATERIALS

www.acsanm.org Article

Wearable Self-Powered Pressure-Sensing Device Based on a Combination of Carbon Nanotubes/Porous Poly(dimethylsiloxane) and Poly(ethylene oxide)

Changwoo Cho, Chaeeun Lee, and Je Hoon Oh*

Cite This: *ACS Appl. Nano Mater.* 2024, 7, 5040−5050 Read Online

ACCESS | Metrics & More | Article Recommendations | Supporting Information

ABSTRACT: The development of technologies such as artificial intelligence and the Internet of Things has increased the demand for wearable, self-powered pressure sensors. Triboelectric nanogenerator (TENG)-based self-powered pressure sensors have emerged as a solution to meet this demand. However, the measurement of static and small pressure ranges remains a challenge. In this paper, we propose a self-powered pressure-sensing device based on the combination of carbon nanotube (CNT)/porous poly(dimethylsiloxane) (PDMS) composite and poly(ethylene oxide) (PEO) film. The proposed device could continuously and reliably measure static and small-range pressure through capacitive pressure sensing while harvesting energy based on the triboelectric effect. The device exhibited a remarkable sensitivity of 1.37 kPa^{-1} due to the incorporation of high-*k* materials (i.e., CNTs, a nanosized filler) in its porous structure and dielectric layer. It also had a power density of 15 mW/m^2 due to the triboelectric interaction between PDMS and PEO. Finally, the fabricated device was connected to a microcontroller unit to perform energy harvesting and pressure sensing simultaneously, demonstrating its great potential as a wearable device.

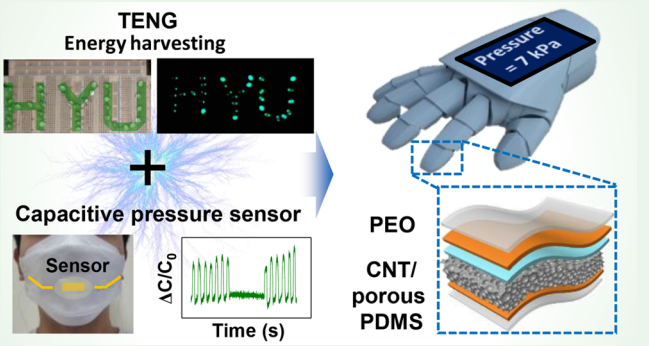

KEYWORDS: *capacitive pressure sensor, triboelectric nanogenerator (TENG), self-powered device, dual-functionality, porous PDMS, carbon nanotube (CNT)*

1. INTRODUCTION

The development of cutting-edge technologies, together with innovative technologies in artificial intelligence, including smart portable/wearable devices[1,2] and artificial electronic skin,[3,4] has promoted research on wearable pressure sensors that establish a connection between the human senses and machines. The advantages of these sensors include high sensitivity, low weight, low cost, and durability.[5,6]

Capacitive-type pressure sensors are more likely to be applied in a variety of fields compared with other types of pressure sensors (e.g., piezoelectric,[7,8] triboelectric,[9,10] and resistive[11,12]) because of their low power consumption, simple structure, and static and low-pressure measurements.[13−15] Capacitive pressure sensors have a sandwich structure with upper and lower electrodes enclosing a dielectric layer. Because the thickness of the dielectric layer changes as external pressure is applied, the capacitance also changes. This process is based on the principle that the thickness of the dielectric layer decreases under pressure, resulting in a corresponding change in capacitance. As a result, a highly deformable dielectric layer has an effect on the sensitivity of capacitive pressure sensors.

Several studies have applied poly(dimethylsiloxane) (PDMS) as a dielectric layer for capacitive pressure sensors owing to its high deformability that stems from its low Young's modulus and exceptional flexibility. PDMS is ideal for wearable devices because of its biocompatibility with the human body.[16,17] However, the low sensitivity of solid-bulk PDMS-based capacitive pressure sensors in practical applications must be addressed.

There are two primary approaches to enhancing the sensitivity of capacitive pressure sensors, which use PDMS as the dielectric layer. First, microstructures such as micropores, microdomes, micropyramids, and microcolumns can be generated within the bulk PDMS dielectric layer to enhance its deformability and sensitivity. Simultaneously, as pressure is applied to the dielectric layer, the low permittivity of air is replaced with the permittivity of the PDMS, leading to greater capacitance changes. The second approach involves the use of

Received: December 4, 2023
Revised: February 2, 2024
Accepted: February 5, 2024
Published: February 23, 2024

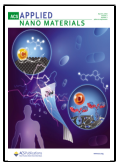

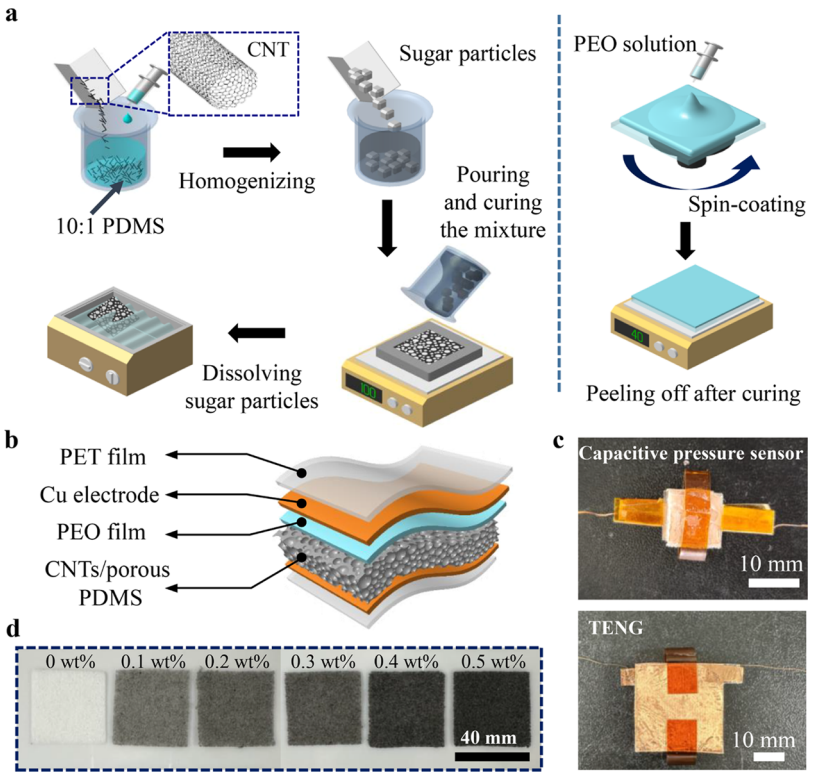

Figure 1. (a) Schematic of the fabrication process of CNT/porous PDMS and the PEO film. (b) Illustration of fabricated self-powered capacitive pressure sensor. (c) Optical features of the capacitive pressure sensor (top) and TENG (bottom) fabricated for evaluation in the proposed self-powered pressure sensor. (d) Optical images of CNT/porous PDMS with CNT concentrations of various weight percent.

PDMS composites containing high-k or high-conductivity nanosized materials, such as carbon nanotubes (CNTs),[18,19] Ag nanowires,[20,21] $BaTiO_3$,[22,23] and zinc oxide.[24,25] Incorporating a small quantity of high-k or high-conductivity nanomaterial into the composite leads to high dielectric constants that significantly enhance the sensitivity of capacitive pressure sensors.

Numerous studies have been conducted to increase sensitivity by combining the above-mentioned two methods. Liu et al. proposed a composite of Ag nanoparticles and porous PDMS using ammonium bicarbonate (NH_4HCO_3) as the foaming agent to improve the sensitivity of the sensor.[26] Ha et al. dip-coated a nickel foam in an Ecoflex-CNT solution and then etched it to fabricate a CNT-porous structured elastomer with a high sensitivity of 3.13 kPa^{-1} at 0−1 kPa.[14] However, despite these attempts to improve sensitivity, their practical application is hindered by the need to constantly charge the power source that drives wearable devices.

In recent years, the triboelectric nanogenerator (TENG) has gained increased attention as a strong power source owing to its ability to convert mechanical movements from the surrounding environment into electrical signals.[27−29] Consequently, TNEG-based pressure sensors have been investigated as self-powered pressure sensors that can detect signals without an external power source.[30,31] However, pressure sensors based on a TENG are not suitable for use as wearable pressure sensors that necessitate the detection of small pressure ranges and static pressure. This limitation arises from their inherent capability to measure only large and impulsive pressures.[32,33] Therefore, real-life wearable pressure sensors should be self-powered and capable of measuring both static and small-range pressures.

In this paper, we propose a wearable self-powered pressure-sensing device based on a CNT/porous PDMS and poly(ethylene oxide) (PEO) combination with dual-functional applications of pressure sensors and energy harvesters. The sensitivity of the fabricated device was improved by enhancing the deformability using a dielectric layer of porous PDMS combined with CNTs as the high-k material. Furthermore, we consider the strong negative triboelectric properties of PDMS and introduce PEO as a positive triboelectric material.[34,35] The proposed device demonstrates its potential as a wearable pressure sensor by reliably and consistently measuring both the static and the small pressure range. Furthermore, when friction was applied to the device, a stable electrical signal was generated, demonstrating its efficacy as an excellent energy source. Finally, by integration of a capacitive pressure sensor and a TENG, a dual-function integrated system was developed that enables pressure sensing and energy harvesting at the same time. We connected the proposed device by attaching it to the fingertip and palm of an integrated system equipped with a microcontroller unit (MCU), and the device successfully harvested energy and measured pressure, showing its potential as a wearable self-powered pressure sensor.

2. EXPERIMENTAL SECTION

2.1. Preparation of Dielectric Layers. Figure 1a shows a schematic of the fabrication process of the dielectric layer. The first step is the fabrication of the CNT/porous PDMS composite by adding CNTs to the PDMS solution at a mass ratio of 0.1:0.5, and mixing in a homomixer for 6 min (ARE-310, Thinky Co.). During the mixing process, the CNT/PDMS solutions were mixed at a speed of 2000 rpm for 4 min and 30 s in the mixing process. Subsequently, a vacuum process is employed for a duration of 1 min and 30 s. The CNT/PDMS solution contained a prepolymer and curing agent in a

https://doi.org/10.1021/acsanm.3c05793
ACS Appl. Nano Mater. 2024, 7, 5040−5050

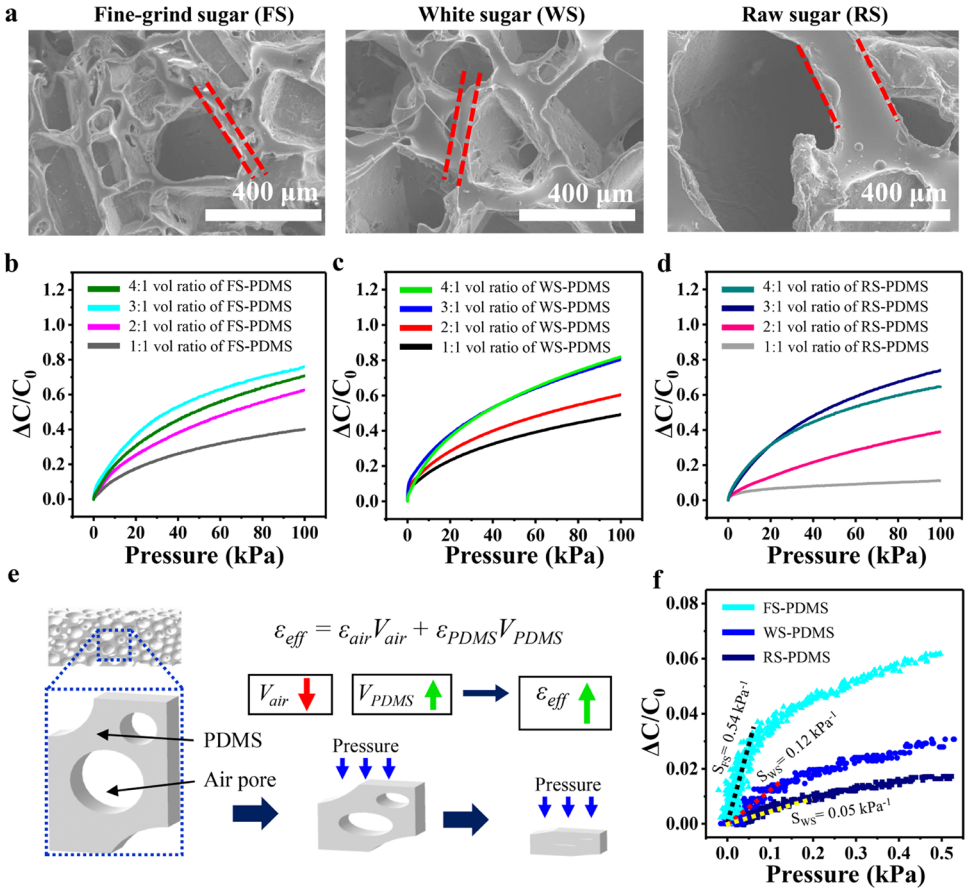

Figure 2. (a) SEM images of porous PDMS using various sugars as sacrificial particles. Capacitance variation graph of sugar−porous PDMS: (b) FS-PDMS, (c) WS-PDMS, and (d) RS-PDMS. (e) Structural change of porous PDMS under compressive load. (f) Comparison of the sensitivity of a porous PDMS capacitive pressure sensor with a 3:1 sugar−PDMS volume ratio with different sizes of sugar applied.

ratio of 10:1. Sugar, which served as the sacrificial particle for the porous structure, was selected in various sizes. The sacrificial particles selected were fine-grained sugar (FS), white sugar (WS), and raw sugar (RS), with sizes of approximately 200, 500, and 700 μm, respectively. Among them, the WS was filtered through a 500 μm mesh to obtain a uniform size.

Sugar was added to the prepared PDMS solution at various volume ratios, from 1:1 to 4:1. The process of mixing sugar into the CNT/PDMS solution was performed manually to avoid curing due to frictional heat caused by the sugar. The mixture was poured into a 40 mm × 40 mm × 1 mm mold and cured on a hot plate at 100 °C for 35 min. Afterward, the cured mixture was rinsed for 3 h in deionized (DI) water using a sonicator to etch the sugar particles and then dried at 60 °C for 1 h to remove the remaining DI water in the CNT/porous PDMS.

The second step is the PEO film fabrication process. PEO powder was dissolved in DI water at 9% (w/w) by using a magnetic stirrer for 12 h. The PEO solution was spin-coated onto a glass substrate at rotational speeds of 500−1500 and 250 rpm intervals for 10 s to obtain various thicknesses and then dried on a hot plate at 50 °C for 3 h. Finally, the PEO film was obtained by peeling it off of the glass substrate.

2.2. Fabrication of a Self-Powered Pressure-Sensing Device. The CNT/porous PDMS composite and the PEO film were cut in to size of 10 mm × 10 mm and 30 mm × 30 mm for evaluation of the capacitive pressure sensor and TENG, respectively. The thickness of CNT/porous PDMS is 1 mm, which is the same as the thickness of the mold used for fabrication. A copper tape with an adhesive on one side was cut into the same size and used as an electrode. The CNT/porous PDMS composite and the PEO film were attached to the adhesive surfaces of the upper and lower electrodes. Then, copper wires were bonded to the top and bottom electrodes by using copper tape. Finally, the self-powered capacitive pressure sensor with the CNT/porous PDMS composite and the PEO film was completed by covering the outer surfaces of both electrodes with a poly(ethylene terephthalate) film to shield them. A schematic of the self-powered pressure-sensing device is shown in Figure 1b. Figure 1c shows the self-powered pressure-sensing device fabricated to be evaluated as a pressure sensor and a TENG, respectively. The measurement and characteristics of the fabricated sensors are described in the Supporting Information.

3. RESULTS AND DISCUSSION

3.1. Capacitive Properties of the CNT/Porous PDMS in a Self-Powered Pressure-Sensing Device. Figure 2a shows scanning electron microscopy (SEM) images of porous PDMS using various sugars as sacrificial particles. The pore sizes of the produced porous PDMS all have the same volume ratio but increase in the order of FS, WS, and RS in proportion to the size of the sugar particles. Additionally, the thickness of the PDMS wall between pores also tended to increase.

Figure 2b−d shows the capacitance variations of a capacitive pressure sensor using porous PDMS as a dielectric layer using FS, WS, and RS, respectively. The number of pores increases as the ratio of sugar increases, while their sizes remain similar to each other. As the sugar content increased, Young's modulus of porous PDMS tended to decrease.[16] The sensitivity of the capacitive pressure sensor is defined as $S = \delta(\Delta C/C_0)/\delta P$, where ΔC is the capacitance variation, C_0 is the initial capacitance when there is no pressure, and P is the applied

https://doi.org/10.1021/acsanm.3c05793
ACS Appl. Nano Mater. 2024, 7, 5040−5050

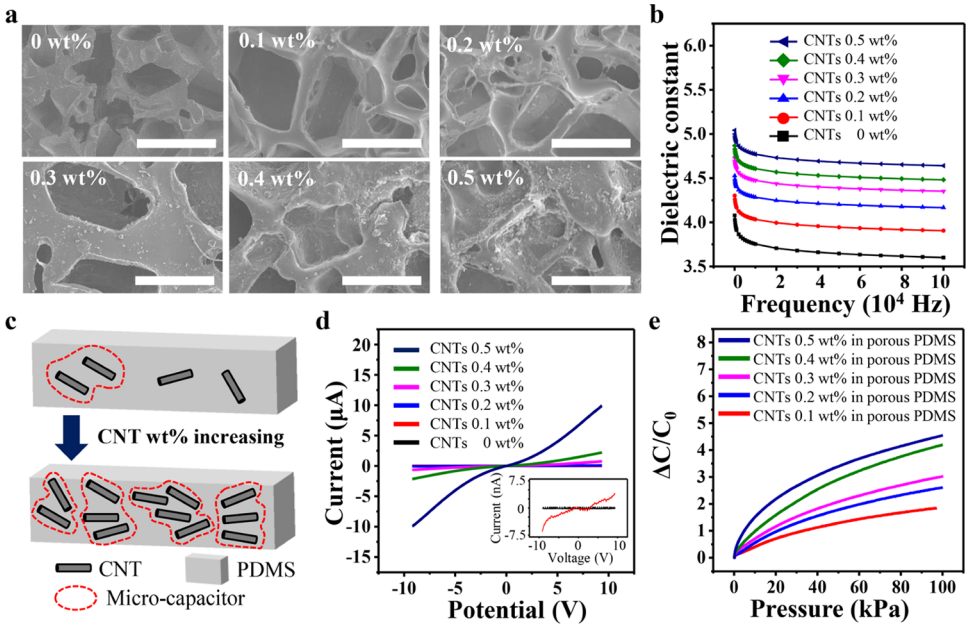

Figure 3. (a) SEM images showing the increasing amount of CNTs in CNT/porous PDMS depending on the weight percentage of CNTs. (b) Dielectric constant for various CNT wt %. (c) Illustration of a microcapacitor that increases as the weight percent of CNTs in PDMS increases. (d) *I*−*V* characteristics of CNT/PDMS composite for various CNT wt %. (e) Capacitance variation graphs of CNT/porous PDMS-based pressure sensors with dielectric layers of different CNTs concentrations in wt %.

pressure. In other words, the larger the change in capacitance and the smaller the initial capacitance, the greater the sensitivity. The sensitivity of the sensor tended to increase as the volume ratio of the sacrificial particles increased due to the increase in porosity. In the capacitive pressure sensors, the definition of capacitance is as follows

$$C = \varepsilon_{air}\varepsilon_r \frac{A}{d} \tag{1}$$

where ε_{air} is the dielectric constant of air in the pores, ε_r is the dielectric constant of the dielectric layer, A and d are the area and the distance between the two electrodes, respectively.[13] Porous PDMS, due to its numerous air-filled pores, exhibits greater susceptibility to deformation under equivalent external pressure in comparison to solid PDMS. Manipulating the sugar ratio led to heightened porosity, decreasing Young's modulus of the dielectric layer and augmenting its deformability. The enhanced capacitance variation, attributed to increased sugar ratio, stems from the transition from low dielectric constant pores ($\varepsilon_{air} = 1$) to the higher dielectric constant of the PDMS matrix ($\varepsilon_{PDMS} = 2.7$) as pores close under pressure. The effective dielectric constant of porous PDMS, ε_{eff} is expressed as

$$\varepsilon_{eff} = V_{air}\varepsilon_{air} + V_{PDMS}\varepsilon_{PDMS} \tag{2}$$

where V_{air} and V_{PDMS} are the volume fractions of air and PDMS, respectively. When pressure is applied, the pores of the dielectric layer are closed, the PDMS volume fraction increases, and the low dielectric constant of air is replaced by the high dielectric constant of PDMS. As a result, the effective dielectric constant of the porous PDMS and the capacitance variation increased compared with those of the bulk PDMS (Figure 2e).

Although different sizes of sacrificial particles were used to fabricate porous PDMS, all three types, FS, WS, and RS, showed the greatest capacitance variation at 3:1 sugar−PDMS volume ratio. The capacitance change of 4:1 sugar−PDMS was similar to or tended to decrease compared to the 3:1 sugar−PDMS volume ratio. The porous PDMS capacitive pressure sensors with a sugar−PDMS volume ratio of 4:1 have a smaller initial capacitance because they contain more pores than those with a 3:1 volume ratio. However, because the volume fraction of PDMS was small, it did not lead to much capacitance change when pressure was applied to the sensor (Table S1 in Supporting Information).

Therefore, we compared the sensitivities of porous PDMS capacitive pressure sensors with a volume ratio of 3:1, which had the largest capacitance change among FS, WS, and RS sacrificial particles (Figure 2f). The sensitivity was observed to be 0.54, 0.12, and 0.05 kPa^{-1} in the order of FS, WS, and RS porous PDMS sensors, respectively. This is because the buckling load of the PDMS walls between the pores is different when compression is applied to the fabricated porous PDMS. Based on Euler's theory of the column buckling, the critical load P_{cr} is calculated as follows

$$P_{cr} = \frac{\pi^2 EI}{(KL)^2} \tag{3}$$

Therefore, the critical load is proportional to the product of the cross-sectional area moment of inertia (I) of the column and the Young's modulus (E) of the column material and inversely proportional to the square of the column length (L). K is the effective length factor.

As the size of the sugar particles decreases, the thickness of the PDMS wall, which acts as a column, decreases. Therefore, the buckling load on the PDMS wall also decreases as the size of the sugar particles decreases, resulting in more deformation for the same force and leading to a higher capacitance change. In contrast to the magnitude of sensitivity, the range of sensitivity was narrower for FS, WS, and RS. This is due to the difference in the volume fraction of pores and PDMS in each pressure sensor as pressure is applied. The smaller the pore

https://doi.org/10.1021/acsanm.3c05793
ACS Appl. Nano Mater. 2024, 7, 5040−5050

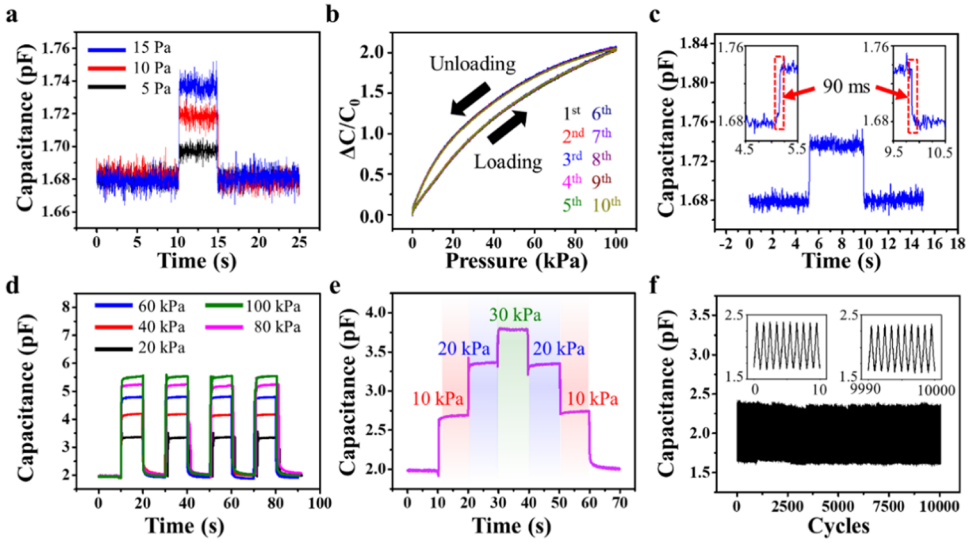

Figure 4. Sensing performance of self-powered pressure-sensing device employing optimized conditions of CNT/porous PDMS and the PEO film. (a) Capacitance changes when applying 5, 10, and 15 Pa pressure to the sensor. (b) Capacitance variation of the sensor under external pressure during 10 consecutive repeated loading and unloading cycles. (c) Response and recovery times of the sensor. (d) Change in capacitance of the sensor at different static pressures. (e) Capacitance change of the sensor under static stepwise pressure. (f) 10,000 cycles of repeated loading and unloading cyclic tests.

size, the more compression is generated for the same force, causing the pore to close faster, resulting in a narrower sensitivity range. Finally, we chose WS porous PDMS, which lies in the middle through a compromise between sensitivity and a linear range. The sensitivity was observed to 0.02, 0.07, and 0.12 kPa^{-1} in WS sugar−PDMS volume ratios of 1:1, 2:1, and 3:1, respectively. In addition, we calculated the porosity of the porous structure based on the volume ratio of sugar−PDMS.[36] The calculated porosity was 50, 66.25, and 75% for WS sugar−PDMS volume ratios of 1:1, 2:1, and 3:1 porous PDMS, respectively.

The sensitivity of capacitive pressure sensors can be enhanced by introducing high-k materials in nanosized form with elevated dielectric constants through percolation into a porous dielectric layer. Figure 3a shows SEM images of WS porous PDMS with different CNT weight percentages. The size of the inner scale bar is 500 μm. In the 0 wt % WS porous PDMS, only pores and PDMS walls were observed, as no CNTs were included. Furthermore, an increase in the amount of aggregated CNTs was observed as the CNT concentration increased. Although there was some agglomeration of CNTs, we were able to produce CNT/porous PDMS using a homomixer with less agglomeration than powdered CNTs. Although there was some agglomeration of CNTs, we were able to produce CNT/porous PDMS using a homomixer with less agglomeration than powdered CNTs. As shown in Figure S2, it was confirmed that powder-type CNTs were entangled in the form of long fillers with the same nanometer-level diameter.

Additionally, we fabricated multiple samples to determine the effect of agglomerated CNTs and checked their reproducibility (Figure S3 in the Supporting Information). The capacitive pressure sensor using the 0.2 wt % CNT/porous PDMS dielectric layer fabricated using the mixing machine showed no significant difference in performance, demonstrating the dispersing ability.

Figure 3b shows the dielectric constant of CNT/PDMS with different CNT weight percentages. As the concentration of CNTs increases, the composite has a higher dielectric constant. The augmentation of the dielectric constant in response to elevated CNT concentration is attributable to the microcapacitor effect, which is the increase in the dielectric constant reaching the percolation threshold.[37,38] Figure 3c illustrates the mechanism by which the dielectric constant of the composite increases as the concentration of CNTs in the CNT/PDMS composite increases. As the concentration of CNTs increases, the CNT network within the composite expands with each CNT acting as an electrode. Therefore, the polymer between the CNTs acts as a dielectric layer, ultimately increasing the number of microcapacitors and contributing to the improvement of the dielectric constant.[39,40]

Consequently, the behavior of the dielectric constant in CNT/PDMS composites can be elucidated through the percolation theory. This is attributed to the pivotal role of microcapacitor formation, which is intrinsically dependent on the concentration of CNTs within the composite.[41,42]

$$\varepsilon \propto (P_c - P)^{-S}, \quad \text{for } P < P_c \tag{4}$$

where ε is the dielectric constant, P is the mass ratio of CNTs, P_C is the percolation threshold, and S is the critical index of the dielectric constant. When the filling of CNTs in the composite is below the percolation threshold, the dielectric properties increase in proportion with the filling concentration, forming microcapacitors.

In addition, the synergy between the large specific surface area and high electrical conductivity of CNTs can provide an infiltration network for charge carrier transport and effectively transport charge carriers. Therefore, the greater the amount of CNTs in CNT/PDMS composites, the greater the amount of energy that can be stored, resulting in a large dielectric constant.[43] However, despite the capacitance contribution of CNTs, conductive fillers increase the field intensity between neighboring fillers, resulting in leakage currents.[44]

Figure 3d shows the relationship between the current flowing through the PDMS containing the CNT and the applied voltage. The higher the concentration of CNTs, the

https://doi.org/10.1021/acsanm.3c05793
ACS Appl. Nano Mater. 2024, 7, 5040−5050

more current was measured. This indicates that as the concentration of CNTs in the composite increases, a greater amount of current is measured at the applied voltage, indicating that the leakage current increases as the CNT concentration increases. The steep rise from about 5 nA for 0.1 wt % CNTs at 10 V applied to 10 μA for 0.5 wt % CNTs indicates that the increasing concentration of CNTs generates a larger amount of charge carriers and a larger amount of current density, resulting in a larger dielectric constant.[45]

Figure 3e presents a notable enhancement in the sensitivity achieved through the synergistic effect of two approaches aimed at amplifying capacitance change, incorporating a porous structure, and introducing CNTs. The capacitance variation of the CNT/porous PDMS capacitive pressure sensor was greater than that of the porous PDMS sensor. In other words, even with the same 3:1 sugar volume ratio, the larger the CNT content, the greater the capacitance variation owing to the high dielectric constant. In the self-powered pressure-sensing device, PEO film thickness had no discernible effect on the performance of the capacitive pressure sensor. Indeed, the weight percentage of CNTs appears to be the key factor affecting the sensor performance (Figure S4 in the Supporting Information).

The performance of a self-powered pressure-sensing device based on a CNT/porous PDMS was assessed for its potential as a wearable electronic device. The detection limit of the sensor was evaluated by measuring capacitance changes for applied loads of 50 mg (5 Pa), 100 mg (10 Pa), and 150 mg (15 Pa), as shown in Figure 4a. The detection limit was significant for measuring subtle forces from sources such as air, sound waves, and small mechanical vibrations. The sensor effectively detected a low pressure of 5 Pa, showcasing its practical applicability.

Figure 4b presents the capacitance change during loading–unloading cycles from 0 to 100 kPa, repeated 1–10 times. The performance remained unaffected due to the elastic recovery of PDMS, resulting in minimal hysteresis. Response and recovery times of the capacitive pressure sensor were both 90 ms, calculated between 10 and 90% intervals of steady-state capacitance, as shown in Figure 4c and its insets.

Wearable devices need to replicate human skin mechanoreceptors, requiring the ability to differentiate between static and dynamic pressure. Static pressure was assessed by applying various pressures (20, 40, 60, 80, and 100 kPa) to the capacitive pressure sensor in four cycles, each lasting around 10 s (Figure 4d). The measured outputs remained consistent for each pressure level. Additionally, Figure 4e indicates a step-like increase in capacitance response with gradual pressure application, affirming the suitability as a wearable pressure sensor. Robustness is crucial for practical use. The sensor maintained stable output signals for 10,000 cycles at a 1 Hz frequency (Figure 4f), displaying no performance degradation. Various applications of the self-powered capacitive pressure sensors were carried out for practicality with the combination of CNT/porous PDMS and the PEO film (Figure S5 in the Supporting Information).

3.2. Triboelectric Characteristics in a Self-Powered Pressure-Sensing Device. PDMS is widely used as the negative triboelectric layer in TENGs because of its high electron affinity and as the dielectric layer of capacitive pressure sensors.[46,47] Inspired by this, CNT/porous PDMS composites were fabricated as the negative triboelectric layer of TENGs for use as the power supply, and the PEO film was introduced as the positive triboelectric layer. The oxygen functional groups exposed on the PEO surface provided a positive charge, showing excellent bipolarity in the triboelectric series. The C–O–C and –OH chemical bonds of PEO exhibited electron rejection owing to the low electron affinity of the hydrogen atom, which also exhibited positive properties in the triboelectric series.[34,35]

Figure 5a illustrates the operational mechanism of the TENG, based on electrostatic induction and triboelectric

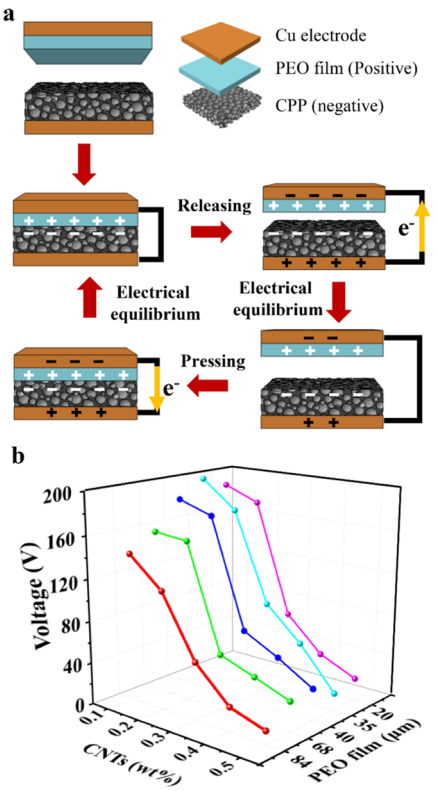

Figure 5. (a) Electricity generation mechanism of the contact–separation mode TENG. (b) The output voltage of CNT/porous PDMS and PEO TENG with different CNT wt % and PEO film thickness.

effects. In the absence of friction, minimal charge transfer between the CNT/porous PDMS and PEO film electrodes occurred. Upon applying external pressure, these materials came into direct contact, inducing a triboelectric effect and charge transfer. Friction between the materials led to charge exchange, resulting in positive and negative charges on the PEO film and CNT/porous PDMS, respectively. Upon pressure release, increased separation intensified the dipole moment. Eventually, charge neutralization ceased electrical output, thus converting mechanical energy into useful electrical power.

We measured the output voltage and short-circuit current of the TENG, which was made from CNT/porous PDMS containing various weight percentages of CNTs, and PEO films of varying thickness at a tapping frequency of 3 Hz. Each point is the average value of the measured value over a period of 1 min (Figure 5b). The output voltage of the TENG decreased as the weight percentage of CNTs increased regardless of the PEO film thickness. This trend can be attributed to the positive triboelectric material properties of the CNTs.[48] As the weight percentage of CNTs increased, the material properties of the

https://doi.org/10.1021/acsanm.3c05793
ACS Appl. Nano Mater. 2024, 7, 5040–5050

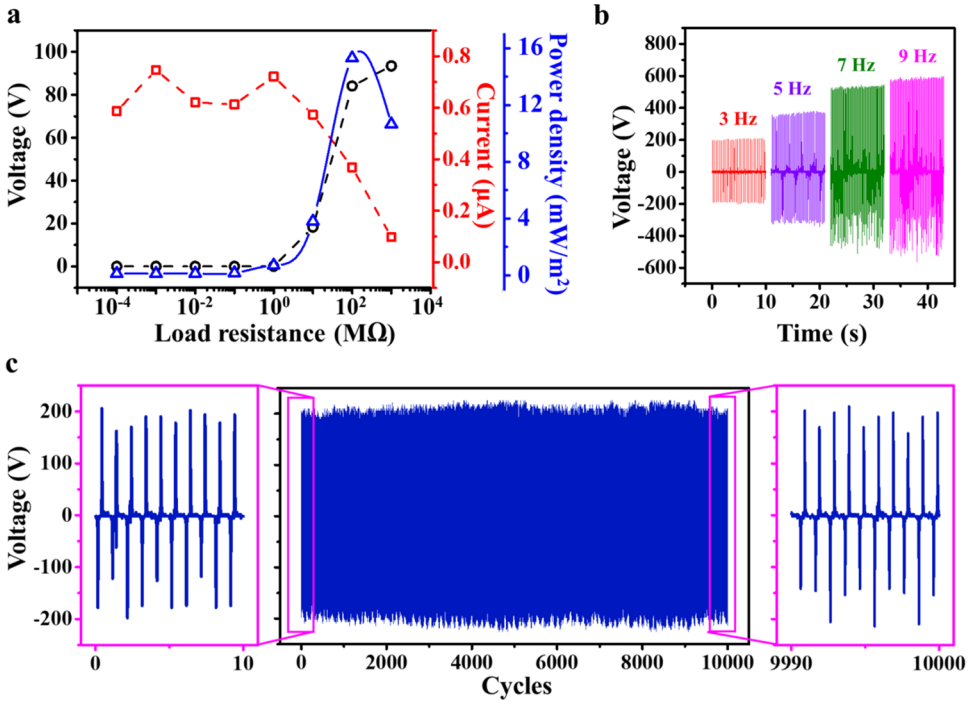

Figure 6. Electrical performances of self-powered pressure-sensing device: (a) voltage, current, and power density, (b) effect of tapping frequency on the output voltage, and (c) energy-harvesting stability test of the device for 10,000 working cycles under 3 Hz.

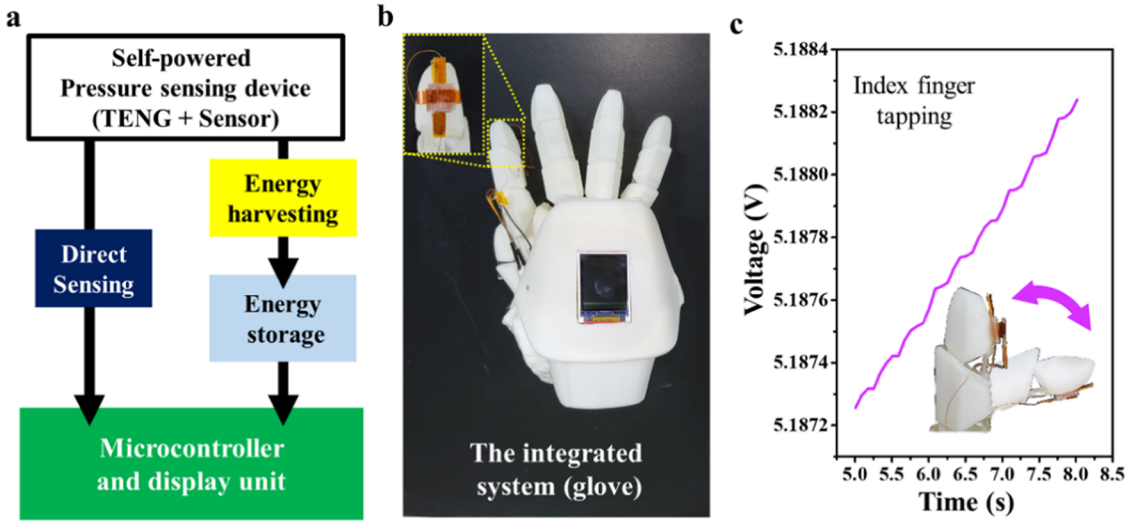

Figure 7. (a) Illustration of an integrated self-powered pressure-sensing system circuit diagram. (b) Self-powered pressure-sensing device attached to the integrated system enables simultaneous pressure sensing and power generation. (c) Energy harvesting enabled by finger tapping.

negative triboelectric material became closer to those of positive materials. Consequently, the gap between CNTs/porous PDMS and PEO in the triboelectric series is reduced, resulting in a decrease in the performance of the TENG.

The electrical performance of the TENG was affected by the PEO film thickness as well as the weight percentage of CNTs in the CNT/porous PDMS. The fabricated TENG showed high performance as the PEO film became thinner, with the highest output voltage of approximately 197 V at 35 μm followed by a lower value at 20 μm. An excessively thick triboelectric layer could increase the distance between the surface of the layer and the electrodes, which ultimately reduced the amount of induced charge. However, if the layer thickness is below a certain threshold, it could generate an insufficient amount of frictional charge.[49,50] The current generated by the fabricated TENG had a nearly constant value, independent of the variations in the CNTs content and PEO thickness (Figure S6 in the Supporting Information).

The high CNT content of the CNT/porous PDMS improved the performance of the capacitive pressure sensor but decreased the electrical performance of the TENG. Therefore, a CNT content of 0.1 wt % was selected by making a trade-off between the sensor and the electrical output of the TENG to optimize the performance of the self-powered pressure sensor.

The power density was measured for practical applications of the TENG. The TENG was connected to a resistor with resistance values ranging from 0.1 kΩ to 1 GΩ. The formula P

https://doi.org/10.1021/acsanm.3c05793
ACS Appl. Nano Mater. 2024, 7, 5040−5050

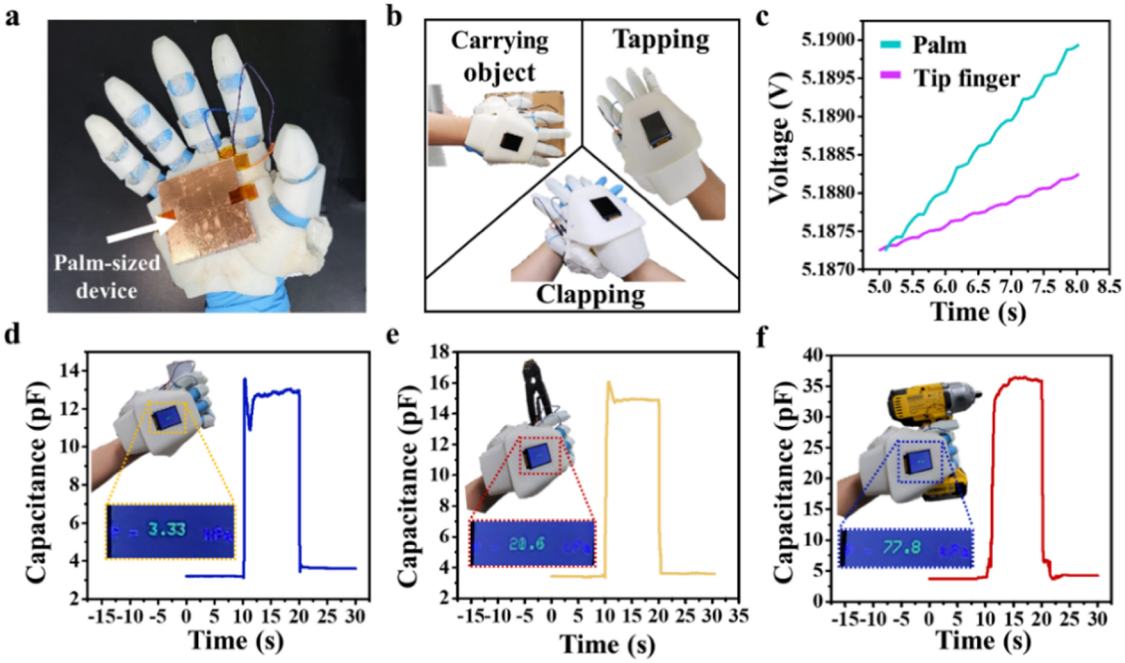

Figure 8. (a) Integrated system with palm-sized (60 mm × 60 mm) CNT/porous PDMS and PEO combination self-powered pressure-sensing device, (b) harvesting energy from a variety of everyday activities (such as clapping, tapping, and carrying objects), (c) comparison of energy harvesting between the index finger and palm size tapping. Pressures of holding various objects: (d) empty can, (e) cutter, and (f) power drill.

$= I^2 \cdot R$ was used to calculate the maximum power density (Figure 6a). The output voltage increased with an increasing load resistance, while the short-circuit current exhibited the opposite trend. The power density rapidly increased between the resistance regions from 0.1 kΩ to 100 MΩ and then decreased at large load resistances. The maximum power density was 15 mW/m^2.

A frequency test was conducted to simulate the diverse frequencies of human movement. As shown in Figure 5b, when the tapping frequency was increased from 3 to 9 Hz, the output voltage remarkably increased from 197 to 598 V. When the friction layers come into contact and then separate at a faster rate, there is a corresponding increase in the flow of electrons seeking equilibrium through the external circuit.[51,52] The proposed TENG also showed good cyclic stability (Figure 6c). It was continuously pressed and released for 10,000 cycles at 3 Hz, showing a nearly constant output voltage of about 200 V during the entire cycle. The performance characteristic of the TENG as a power source was evaluated once again by several confirmatory experiments (Figure S7 and Video S1 in the Supporting Information).

3.3. Applications of an Integrated Pressure-Sensing System. Finally, we fabricated an integrated self-powered pressure-sensing system consisting of CNT/porous PDMS and the PEO film that can be a dual-functionalized device with a capacitive pressure sensor and TENG. A conceptual diagram of the fabricated system is shown in Figure 7a. The dual-functionalized device was connected to an MCU to measure the pressure while charging the energy storage that powered the MCU. A combination of a 7 V lithium-ion battery and 1000 μF was used as the energy storage to drive the MCU used in the application (Figure S8 in the Supporting Information). The measured pressure was calculated in the MCU, and the applied pressure was monitored through a display unit. In this integrated system, the index finger of the glove was equipped with a purpose-built dual-function application device capable of energy harvesting and pressure measurement (Figure 7b). The fabricated self-powered pressure-sensing device can function as both a capacitive pressure sensor and a TENG in one module. However, it is not efficient to perform pressure sensing and energy harvesting at the same time. TENGs can harvest energy by utilizing friction. When measuring small or static pressures, not enough friction is applied and energy harvesting does not occur. Therefore, first, energy can be harvested from the kinetic energy dissipated by friction to help drive the MCU. Sequentially, the pressure applied to the self-powered pressure-sensing device in pressure-sensing mode can be measured and indicated on the display module. When friction is applied to the index finger of the integrated system, the device reliably charges the energy storage (Figure 7c). The integrated system achieved energy harvesting when friction was applied, successfully detected the pressure applied to the index finger of the glove, and displayed it (Video S2 in the Supporting Information).

Furthermore, we noted that the human palm plays an important role in grasping and holding objects, and the pressure on the human palm has many effects on health such as carpal tunnel syndrome.[53,54] Therefore, we applied a palm-sized (60 mm × 60 mm) self-powered pressure-sensing device to the integrated system (Figure 8a). The device in the palm of the integrated system enabled energy harvesting using a large surface area. Figure 8b shows that the fabricated palm-sized device could utilize a variety of everyday frictions such as clapping, palm tapping, and carrying objects. Although the size of the proposed self-powered pressure-sensing device has increased approximately 36 times, its performance has not increased proportionately. Although the palm-sized self-powered pressure-sensing device did not deliver overwhelming performance, it was confirmed that wasted energy could be harvested through various movements using the palm (Figure 8c).

https://doi.org/10.1021/acsanm.3c05793
ACS Appl. Nano Mater. 2024, 7, 5040−5050

Figure 8d–f shows the change in capacitance and the pressure measured by the system when holding various objects, including an empty can, a cutter, and a power drill, respectively. The heavier the weight of the object being held by the integrated system, the more capacitance changes. When holding an empty can, a cutter, and a power drill with the integrated system, the capacitance changes approximately were 9, 12, and 33 μF, respectively, and the pressure on the palm was 3.3, 20.6, and 77.8 kPa, respectively. Therefore, we successfully developed a versatile device by combining CNTs/porous PDMS with a PEO film. This device functions as both a capacitive pressure sensor and a TENG. Demonstrating its potential for energy harvesting and pressure sensing, we applied it to the index finger and palm, highlighting its adaptability for use on various body parts.

4. CONCLUSIONS

In summary, a self-powered capacitive pressure sensor was successfully fabricated by employing a composite structure consisting of a CNT/porous PDMS and a PEO film. The sacrificial particle method utilized in the fabrication process significantly affected the porosity of the structure, which, in turn, influenced the deformability of the dielectric layer. Moreover, the incorporation of CNTs as the high-k nanosized filer material enhanced the dielectric constant of the dielectric layer, resulting in the CNTs/porous PDMS-based pressure sensor with a high sensitivity of 1.37 kPa^{-1}. In addition, since PDMS exhibits negative triboelectric properties, PEO (a strong positive material) was introduced to form a combination of CNT/porous PDMS–PEO film, which was utilized as a power source through the TENG. The optimized TENG had a power density of 15 mW/m^2, and it stably harvested electrical energy under various conditions.

We successfully integrated the capacitive pressure sensor and TENG into a single model by employing CNT/porous PDMS and the PEO film. The integrated model was then affixed to the index finger of a glove and connected to the MCU, which enabled simultaneous energy harvesting and pressure measurements.

■ ASSOCIATED CONTENT

Supporting Information

The Supporting Information is available free of charge at https://pubs.acs.org/doi/10.1021/acsanm.3c05793.

Measurement system of self-powered capacitive pressure sensor, capacitance variation comparison of the sensor with a sugar–PDMS vol ratio of 3:1 and 4:1, the short-circuit current, and capacitance variation of pressure sensors based on different CNTs contents and PEO thickness (PDF)

LED illumination (MP4)

Operation of a glove equipped with a self-powered pressure sensor (MP4)

■ AUTHOR INFORMATION

Corresponding Author

Je Hoon Oh − *Department of Mechanical Engineering and BK21 FOUR ERICA-ACE Center, Hanyang University, Ansan, Gyeonggi-do 15588, Republic of Korea;* orcid.org/0000-0001-5646-3619; Phone: +82314005252; Email: jehoon@hanyang.ac.kr; Fax: +82314004705

Authors

Changwoo Cho − *Department of Mechanical Engineering and BK21 FOUR ERICA-ACE Center, Hanyang University, Ansan, Gyeonggi-do 15588, Republic of Korea*

Chaeeun Lee − *Department of Mechanical Engineering and BK21 FOUR ERICA-ACE Center, Hanyang University, Ansan, Gyeonggi-do 15588, Republic of Korea*

Complete contact information is available at: https://pubs.acs.org/10.1021/acsanm.3c05793

Notes

The authors declare no competing financial interest.

■ ACKNOWLEDGMENTS

This work was supported by the National Research Foundation of Korea (NRF) grant funded by the Korea government (MSIT) (No. 2019R1A2C1005023).

■ REFERENCES

(1) Chen, T.-M.; Tsai, Y.-H.; Tseng, H.-H.; Liu, K.-C.; Chen, J.-Y.; Huang, C.-H.; Li, G.-Y.; Shen, C.-Y.; Tsao, Y. SRECG: ECG Signal Super-resolution Framework for Portable/Wearable Devices in Cardiac Arrhythmias Classification. *IEEE Trans. Consumer Electron.* **2023**, *69* (3), 250–260.

(2) Zhao, Z.; Xia, K.; Hou, Y.; Zhang, Q.; Ye, Z.; Lu, J. Designing flexible, smart and self-sustainable supercapacitors for portable/wearable electronics: from conductive polymers. *Chem. Soc. Rev.* **2021**, *50* (22), 12702–12743.

(3) Neto, J.; Chirila, R.; Dahiya, A. S.; Christou, A.; Shakthivel, D.; Dahiya, R. Skin-Inspired Thermoreceptors-Based Electronic Skin for Biomimicking Thermal Pain Reflexes. *Adv. Sci.* **2022**, *9* (27), No. e2201525.

(4) Niu, H.; Li, H.; Gao, S.; Li, Y.; Wei, X.; Chen, Y.; Yue, W.; Zhou, W.; Shen, G. Perception-to-Cognition Tactile Sensing Based on Artificial-Intelligence-Motivated Human Full-Skin Bionic Electronic Skin. *Adv. Mater.* **2022**, *34* (31), No. e2202622.

(5) Keum, K.; Eom, J.; Lee, J. H.; Heo, J. S.; Park, S. K.; Kim, Y.-H. Fully-integrated wearable pressure sensor array enabled by highly sensitive textile-based capacitive ionotronic devices. *Nano Energy* **2021**, *79*, No. 105479.

(6) Zhou, Q.; Ji, B.; Wei, Y.; Hu, B.; Gao, Y.; Xu, Q.; Zhou, J.; Zhou, B. A bio-inspired cilia array as the dielectric layer for flexible capacitive pressure sensors with high sensitivity and a broad detection range. *J. Mater. Chem. A* **2019**, *7* (48), 27334–27346.

(7) Wei, S.; Qiu, X.; An, J.; Chen, Z.; Zhang, X. Highly sensitive, flexible, green synthesized graphene/biomass aerogels for pressure sensing application. *Compos. Sci. Technol.* **2021**, *207*, No. 108730.

(8) Yang, H.; Shang, J.-C.; Wang, W.-F.; Yang, Y.-F.; Yuan, Y.-N.; Lei, H.-S.; Fang, D.-N. Polyurethane sponges-based ultrasensitive pressure sensor via bioinspired microstructure generated by pre-strain strategy. *Compos. Sci. Technol.* **2022**, *221*, No. 109308.

(9) Lee, K. Y.; Yoon, H. J.; Jiang, T.; Wen, X.; Seung, W.; Kim, S. W.; Wang, Z. L. Fully Packaged Self-Powered Triboelectric Pressure Sensor Using Hemispheres-Array. *Adv. Energy Mater.* **2016**, *6* (11), No. 1502566.

(10) Lin, Z.; Chen, J.; Li, X.; Zhou, Z.; Meng, K.; Wei, W.; Yang, J.; Wang, Z. L. Triboelectric Nanogenerator Enabled Body Sensor Network for Self-Powered Human Heart-Rate Monitoring. *ACS Nano* **2017**, *11* (9), 8830–8837.

(11) Kang, B.-C.; Ha, T.-J. Human-interactive drone system remotely controlled by printed strain/pressure sensors consisting of carbon-based nanocomposites. *Compos. Sci. Technol.* **2019**, *182*, No. 107784.

(12) Zheng, S.; Wu, X.; Huang, Y.; Xu, Z.; Yang, W.; Liu, Z.; Yang, M. Multifunctional and highly sensitive piezoresistive sensing textile based on a hierarchical architecture. *Compos. Sci. Technol.* **2020**, *197*, No. 108255.

(13) Cho, C.; Kim, D.; Lee, C.; Oh, J. H. Ultrasensitive Ionic Liquid Polymer Composites with a Convex and Wrinkled Microstructure and Their Application as Wearable Pressure Sensors. *ACS Appl. Mater. Interfaces* **2023**, *15* (10), 13625−13636.
(14) Ha, K. H.; Zhang, W.; Jang, H.; Kang, S.; Wang, L.; Tan, P.; Hwang, H.; Lu, N. Highly Sensitive Capacitive Pressure Sensors over a Wide Pressure Range Enabled by the Hybrid Responses of a Highly Porous Nanocomposite. *Adv. Mater.* **2021**, *33* (48), No. e2103320.
(15) Sharma, T.; Je, S.-S.; Gill, B.; Zhang, J. X. J. Patterning piezoelectric thin film PVDF−TrFE based pressure sensor for catheter application. *Sens. Actuators, A* **2012**, *177*, 87−92.
(16) Hwang, J.; Kim, Y.; Yang, H.; Oh, J. H. Fabrication of hierarchically porous structured PDMS composites and their application as a flexible capacitive pressure sensor. *Composites, Part B* **2021**, *211*, No. 108607.
(17) Yang, C.-R.; Wang, L.-J.; Tseng, S.-F. Arrayed porous polydimethylsiloxane/barium titanate microstructures for high-sensitivity flexible capacitive pressure sensors. *Ceram. Int.* **2022**, *48* (9), 13144−13153.
(18) Kozinsky, B.; Marzari, N. Static dielectric properties of carbon nanotubes from first principles. *Phys. Rev. Lett.* **2006**, *96* (16), No. 166801.
(19) Mech, B. C.; Kumar, J. Effect of high-kdielectric on the performance of Si, InAs and CNT FET. *Micro Nano Lett.* **2017**, *12* (9), 624−629.
(20) Joo, Y.; Byun, J.; Seong, N.; Ha, J.; Kim, H.; Kim, S.; Kim, T.; Im, H.; Kim, D.; Hong, Y. Silver nanowire-embedded PDMS with a multiscale structure for a highly sensitive and robust flexible pressure sensor. *Nanoscale* **2015**, *7* (14), 6208−6215.
(21) Lim, S.; Oh, J.-M.; Yoo, B.; Han, C. J.; Lee, B.-J.; Oh, M. S.; Kim, J.-W. Transparent and stretchable capacitive pressure sensor using selective plasmonic heating-based patterning of silver nanowires. *Appl. Surf. Sci.* **2021**, *561*, No. 149989.
(22) Ma, L.; Yu, X.; Yang, Y.; Hu, Y.; Zhang, X.; Li, H.; Ouyang, X.; Zhu, P.; Sun, R.; Wong, C.-p. Highly sensitive flexible capacitive pressure sensor with a broad linear response range and finite element analysis of micro-array electrode. *J. Materiomics* **2020**, *6* (2), 321−329.
(23) Wu, W.; Schnittker, K.; Andrews, J. *Printed Capacitive Pressure Sensor with Enhanced Sensitivity through a Layered PDMS/BaTiO3 Structure*; IEEE Sensors, 2021.
(24) Hsieh, G. W.; Ling, S. R.; Hung, F. T.; Kao, P. H.; Liu, J. B. Enhanced piezocapacitive response in zinc oxide tetrapod-poly-(dimethylsiloxane) composite dielectric layer for flexible and ultrasensitive pressure sensor. *Nanoscale* **2021**, *13* (12), 6076−6086.
(25) Wood, G. S.; Jeronimo, K.; Che Mahzan, M. A. B.; Cheung, R.; Mastropaolo, E. Zinc oxide nanowires-based flexible pressure sensor. *Micro Nano Lett.* **2021**, *16* (8), 432−435.
(26) Liu, S.-Y.; Lu, J.-G.; Shieh, H.-P. D. Influence of Permittivity on the Sensitivity of Porous Elastomer-Based Capacitive Pressure Sensors. *IEEE Sens. J.* **2018**, *18* (5), 1870−1876.
(27) Kim, Y.; Wu, X.; Lee, C.; Oh, J. H. Characterization of PI/PVDF-TrFE Composite Nanofiber-Based Triboelectric Nanogenerators Depending on the Type of the Electrospinning System. *ACS Appl. Mater. Interfaces* **2021**, *13* (31), 36967−36975.
(28) Kim, Y.; Wu, X.; Oh, J. H. Fabrication of triboelectric nanogenerators based on electrospun polyimide nanofibers membrane. *Sci. Rep.* **2020**, *10* (1), No. 2742.
(29) Lee, C.; Cho, C.; Oh, J. H. Highly flexible triboelectric nanogenerators with electrospun PVDF-TrFE nanofibers on MWCNTs/PDMS/AgNWs composite electrodes. *Composites, Part B* **2023**, *255*, No. 110622.
(30) Son, J.-h.; Heo, D.; Song, Y.; Chung, J.; Kim, B.; Nam, W.; Hwang, P. T. J.; Kim, D.; Koo, B.; Hong, J.; Lee, S. Highly reliable triboelectric bicycle tire as self-powered bicycle safety light and pressure sensor. *Nano Energy* **2022**, *93*, No. 106797.
(31) Zhang, C.; Liu, L.; Zhou, L.; Yin, X.; Wei, X.; Hu, Y.; Liu, Y.; Chen, S.; Wang, J.; Wang, Z. L. Self-Powered Sensor for Quantifying Ocean Surface Water Waves Based on Triboelectric Nanogenerator. *ACS Nano* **2020**, *14* (6), 7092−7100.
(32) Lin, M.-F.; Xiong, J.; Wang, J.; Parida, K.; Lee, P. S. Core-shell nanofiber mats for tactile pressure sensor and nanogenerator applications. *Nano Energy* **2018**, *44*, 248−255.
(33) Parida, K.; Bhavanasi, V.; Kumar, V.; Bendi, R.; Lee, P. S. Self-powered pressure sensor for ultra-wide range pressure detection. *Nano Res.* **2017**, *10* (10), 3557−3570.
(34) Lin, C.; Zhao, H.; Huang, H.; Ma, X.; Cao, S. PEO/cellulose composite paper based triboelectric nanogenerator and its application in human-health detection. *Int. J. Biol. Macromol.* **2023**, *228*, 251−260.
(35) Ding, P.; Chen, J.; Farooq, U.; Zhao, P.; Soin, N.; Yu, L.; Jin, H.; Wang, X.; Dong, S.; Luo, J. Realizing the potential of polyethylene oxide as new positive tribo-material: Over 40 W/m2 high power flat surface triboelectric nanogenerators. *Nano Energy* **2018**, *46*, 63−72.
(36) Ongari, D.; Boyd, P. G.; Barthel, S.; Witman, M.; Haranczy, M.; Smit, B. Accurate Characterization of the Pore Volume in Microporous Crystalline Materials. *Langmuir* **2017**, *33*, 14529−14538.
(37) Hashemi, R.; Weng, G. J. A theoretical treatment of graphene nanocomposites with percolation threshold, tunneling-assisted conductivity and microcapacitor effect in AC and DC electrical settings. *Carbon* **2016**, *96*, 474−490.
(38) Wang, D.; Zhang, X.; Zha, J.-W.; Zhao, J.; Dang, Z.-M.; Hu, G.-H. Dielectric properties of reduced graphene oxide/polypropylene composites with ultralow percolation threshold. *Polymer* **2013**, *54* (7), 1916−1922.
(39) Song, S.; Xia, S.; Wei, Y.; Lv, X.; Sun, S.; Li, Q. Fluoro-polymer-coated carbon nanotubes for improved interfacial interactions and dielectric properties in MWCNTs/PVDF composites. *J. Mater. Sci.* **2020**, *55* (8), 3212−3227.
(40) Zhang, B.; Tian, G.; Xiong, D.; Yang, T.; Chun, F.; Zhong, S.; Lin, Z.; Li, W.; Yang, W. Understanding the Percolation Effect in Triboelectric Nanogenerator with Conductive Intermediate Layer. *Research* **2021**, *2021*, No. 7189376.
(41) Wang, L.; Dang, Z. Carbon Nanotube Composites with High Dielectirc Comstant at Low Percolation Threshold. *Appl. Phys. Lett.* **2005**, *87*, No. 042903.
(42) Liu, F.; Dai, S.; Cao, J.; Zhang, Z.; Cheng, G.; Ding, J. CNTs based capacitive stretchable pressure sensor with stable performance. *Sens. Actuators, A* **2022**, *343*, No. 113672, DOI: 10.1016/j.sna.2022.113672.
(43) Muchuweni, E.; Mombeshora, E. T.; Martincigh, B. S.; Nyamori, V. O. Recent Applications of Carbon Nanotubes in Organic Solar Cells. *Front. Chem.* **2022**, *9*, No. 733552.
(44) Liu, Z.; Wang, K.; Jiang, X.; Javed, M. S.; Han, W. Overcoming current leaks in CNT/PDMS triboelectric composites by wrapping CNTs with TiO2 insulation layer. *Appl. Phys. Lett.* **2022**, *121* (11), No. 113902, DOI: 10.1063/5.0116090.
(45) Anirban, S.; Roy, R.; Dutta, A. Structure, charge carrier conduction, dielectric properties and leakage current density of Dy2CoMnO6 double perovskite. *J. Alloys Compd.* **2022**, *928*, No. 167184.
(46) Harnchana, V.; Ngoc, H. V.; He, W.; Rasheed, A.; Park, H.; Amornkitbamrung, V.; Kang, D. J. Enhanced Power Output of a Triboelectric Nanogenerator using Poly(dimethylsiloxane) Modified with Graphene Oxide and Sodium Dodecyl Sulfate. *ACS Appl. Mater. Interfaces* **2018**, *10* (30), 25263−25272.
(47) He, W.; Sohn, M.; Ma, R.; Kang, D. J. Flexible single-electrode triboelectric nanogenerators with MXene/PDMS composite film for biomechanical motion sensors. *Nano Energy* **2020**, *78*, No. 105383.
(48) Wang, H.; Shi, M.; Zhu, K.; Su, Z.; Cheng, X.; Song, Y.; Chen, X.; Liao, Z.; Zhang, M.; Zhang, H. High performance triboelectric nanogenerators with aligned carbon nanotubes. *Nanoscale* **2016**, *8* (43), 18489−18494.
(49) Hasan, S.; Kouzani, A. Z.; Adams, S.; Long, J.; Mahmud, M. A. P. Comparative study on the contact-separation mode triboelectric nanogenerator. *J. Electrost.* **2022**, *116*, No. 103685.

(50) Kang, X.; Pan, C.; Chen, Y.; Pu, X. Boosting performances of triboelectric nanogenerators by optimizing dielectric properties and thickness of electrification layer. *RSC Adv.* **2020**, *10* (30), 17752−17759.
(51) Wang, X.; Yang, B.; Liu, J.; Zhu, Y.; Yang, C.; He, Q. A flexible triboelectric-piezoelectric hybrid nanogenerator based on P(VDF-TrFE) nanofibers and PDMS/MWCNT for wearable devices. *Sci. Rep.* **2016**, *6*, No. 36409.
(52) Xiong, J.; Cui, P.; Chen, X.; Wang, J.; Parida, K.; Lin, M. F.; Lee, P. S. Skin-touch-actuated textile-based triboelectric nanogenerator with black phosphorus for durable biomechanical energy harvesting. *Nat. Commun.* **2018**, *9* (1), No. 4280.
(53) Kubo, K.; Cheng, Y. S.; Zhou, B.; An, K. N.; Moran, S. L.; Amadio, P. C.; Zhang, X.; Zhao, C. The quantitative evaluation of the relationship between the forces applied to the palm and carpal tunnel pressure. *J. Biomech.* **2018**, *66*, 170−174.
(54) Li, Y.; Tao, R.; Li, Y.; Yang, Y.; Zhou, J.; Chen, Y. A Highly Adaptive Robotic Gripper Palm with Tactile Sensing. In *2022 IEEE International Conference on Real-time Computing and Robotics (RCAR)* 2022; pp 130−135.

https://doi.org/10.1021/acsanm.3c05793
ACS Appl. Nano Mater. 2024, 7, 5040−5050